

Generalized interfaces

D. K. Ferry,^{a)} R. A. Akis, J. P. Bird, M. Elhassan, I. Knezevic, C. Prasad, and A. Shailos
Department of Electrical Engineering and Center for Solid State Electronics Research, Arizona State University, Tempe, Arizona 85287-5706

(Received 19 January 2003; accepted 24 February 2003; published 5 August 2003)

The properties of very small semiconductor devices can be dominated by their environments in a nonperturbative manner. General treatments of the device embedded within its environment must account for the strong interactions between the device and the environment. While perturbative examples include remote phonons, surface roughness scattering, and edge fluctuations, the more general class give new dynamics for the device. This includes superlattice effects in arrays of devices and modified dynamics arising from device induced variations in the environment. © 2003 American Vacuum Society. [DOI: 10.1116/1.1588642]

I. INTRODUCTION

Over the past few decades, industry has continuously pushed the size of an individual semiconductor device ever smaller, and research devices have passed the 10 nm scale. The development of other nano-structured “devices” has fostered the current fashion for “nanotechnology.” Yet, the study of sub-100 nm semiconductor devices has been supported for more than 25 yr by the Department of Defense through the original Ultra-Small Electronics Program, established in 1977. Essential elements for today’s small semiconductor devices were discussed already at the beginning of this program, and a processing detail for a 25 nm silicon-based field-effect transistor (FET) was put forward.¹ Of more interest was a theoretical development, in which it was pointed out that the central feature of transport in such very small devices, is that the device microdynamics cannot be treated in isolation but must be considered in conjunction with its environment. That is, any single device is embedded within an “environment” which consists of its own interfaces and the array of other devices to which it is connected, either by design or by accident.²

In this article, we will review this theoretical development, but put it into context with more recent experimental developments, both for devices and for quantum structures which may find usefulness in the next generations of signal processing circuitry. In Sec. II we outline the general treatment of expanding the density matrix for the entire system in a manner which allows one to pull out the critical dynamics of the buried system of interest. We then talk about the role of interfaces and coherent device–device interactions, particularly as regards a superlattice of devices. Examples of early work in lateral surface superlattices and more current work on arrays of open quantum dots are then discussed to show how individual device dynamics are significantly modified when these latter are coupled to their environment and/or other devices.

^{a)}Author to whom correspondence should be addressed; electronic mail: ferry@asu.edu

II. EMBEDDED DEVICE

Let us consider an arbitrary small “device” which is embedded within a larger environment. Normally, in quantum transport, the kinetic equations are developed for the larger closed system so that conservation laws may be invoked. In fact, however, we are interested in the small “system,” represented by the device, which is open to the larger environment and in which the flow of energy into, and out of, the device are by quite different processes. In general, we may write the total Hamiltonian as $H_T = H_d + H_e + H_{ed}$, where the terms represent the device, the remaining environment, and the interaction between the device and its environment. From the Liouville equation for the total density matrix, it is possible to introduce a projection operator, which separates out that part of the Hamiltonian that acts on the device, and to write quite generally¹

$$i\hbar \frac{\partial \rho_d}{\partial t} = [H_d, \rho_d] + \text{Tr}_e\{[H_{ed}, \rho_T]\}, \quad (1)$$

and it is the last term that causes significant coupling. Here, the trace is carried over the environment variables, and $\rho_d = \text{Tr}_e\{P\rho_T\}$ gives the “device” density matrix, where P is the projection operator (in general, a superoperator). One wants to have an equation for the device density matrix only, so that manipulations of this last term must be performed. These lead to¹

$$i\hbar \frac{\partial \rho_d}{\partial t} = \hat{H}_d \rho_d + \langle \hat{H}_{ed} \rangle \rho_d + \hat{\Sigma}(0) \rho_d, \quad (2)$$

where

$$\langle \hat{H}_{ed} \rangle \rho_d \equiv \text{Tr}_e\{\hat{P}\hat{H}_{ed}\hat{P}\rho_T\} \quad (3)$$

provides the coupling to the environment, and the last term is a non-Hermitian operator of the gain–loss type which comprises an irreversible part of the kinetic equation for the device. Here, the caret indicates a (commutator generating) superoperator.³

The environment term in Eq. (2) is essentially a time-reversible component which is a modification of device dynamics. Hence, the coupling of the device to the environment provides both a dissipative term and a nondissipative, but

renormalizing term. The dissipative term can involve remote phonons,^{4,5} as well as interface roughness scattering at junctions between dissimilar material.^{6,7} The nondissipative term can lead to size quantization,⁸ but also to cooperative effects among the multiple devices in the array.⁹ An important aspect of this renormalization is that it is possible to choose a *preferred* basis set for the embedded device, utilizing the fact that the eigenvalues of the projection operator are either 0 or 1.¹⁰ This means that the proper basis functions will include directly a correction for the interaction with the environment—they will not be the basis functions of the isolated device! This will be clearly important in our discussion below of open quantum dots.

III. BOUNDARY EFFECTS

In general, the development of the theory of transport in Si metal–oxide–semiconductor FETs (MOSFETs) clearly expresses the role of the mobility, but ignores most other effects that arise from scattering processes which arise from regions other than the channel of the device. The dependence upon the mobility led to the early recognition that surface-roughness scattering, arising from a random position of the actual interface between the silicon and the oxide, would be quite important in devices with large inversion densities.⁶ Indeed, it is generally accepted today that this scattering will dominate the mobility in small MOSFETs.¹¹ What has not been so clearly recognized is that this scattering is only one of the multitude of environmental scattering effects that become important in such small devices.

The carriers in the channel are located quite close to the interface with the oxide. Silicon dioxide is a polar material, and the dielectric discontinuity at the interface leads to localized interface polar modes, which can scatter the carriers.⁴ In addition, the polar modes of the oxide itself can scatter the carriers even though they are more remote.¹² Moreover, the high density of carriers in the drain can also lead to a “remote” scattering of the carriers in the channel through the electron–electron interaction.¹³

Surface-roughness scattering arises from a dissipative effect of the random potential at the interface. There can be many other sources of a random potential, and most of these will lead to further important effects in small devices. For example, the gate is fabricated as a fine polysilicon line, and edge roughness in this line will affect the device performance.¹⁴ This has been extensively studied in device simulations, where the importance of this effect has been verified.¹⁵ Another source of a random potential lies in variations in the thickness of the oxide itself.¹⁶ In fact, the top surface of the oxide, where it joins the polysilicon gate, is a rougher version of the lower interface. While the latter is responsible for surface-roughness scattering, the presence of both top- and bottom-surface roughness means that there is a random variation in the thickness of the oxide. This, in turn, leads to a random variation in the surface potential and in the inversion density. While the scattering due to the lower surface variations has been recognized, the importance of the

density variations on device performance are only now being investigated.

IV. LATERAL SUPERLATTICES

The results of Eq. (2) led to the conclusion that a device, which was embedded in a regular array of similar devices, could exhibit superlattice behavior. In two dimensions, the nature of lateral superlattices were discussed by Hofstadter some years ago.¹⁷ When a magnetic field is present, the trajectories curve around a two-dimensional torus, representing periodicity in the two dimensions. Only when the wraps around the torus, in these two dimensions, are rationally related do the trajectories close on themselves and allow solutions to the Schrödinger equation. Hence, the new version of this on a discrete lattice of size a is given by the Harper equation¹⁸

$$\psi(n+1) + \psi(n-1) + 2 \cos(2\pi n\alpha - \nu)\psi(n) = \varepsilon\psi(n), \quad (4)$$

where $x = na$, the energy is $\varepsilon = 2E/V_0$, where V_0 is the amplitude of the periodic potential, and the rationalized number of flux quanta per cell is

$$\alpha = \frac{eBa^2}{h}. \quad (5)$$

The need for a to be a rational number means that the spectrum in the (new) two-dimensional space (E, B) is fractal, but more importantly it must be periodic in both magnetic field and in energy. The amount of this periodicity is $\Delta B = h/ea^2$ and $\Delta E = 4V_0$.

Many experimental studies have probed the nature of magnetotransport in such lateral superlattices, and these previously have been reviewed.¹⁹ Here, we discuss two observations which clearly illustrate that the Hofstadter butterfly, the spectrum of eigenvalues mentioned above, can be seen in experiments through the new periodicities that this spectrum enforces upon the transport. In high mobility samples of GaAs/AlGaAs heterostructures, the observation of the quantum Hall effect is modified by the presence of the superlattice potential [seen in the inset of Fig. 1(b), here with a periodicity of 160 nm]. This leads to a set of oscillatory magnetoconductance at the edges of the Hall plateaus.²⁰ This occurs only at the edges, where the Fermi energy lies in the Landau level in the bulk of the material (on the plateaus, the Fermi energy lies in the edge states and these channels do not feel the potential). The oscillations correspond to the addition/deletion of two electron per unit cell of the superlattice as the magnetic field or gate voltage (energy) is swept.²¹

A more interesting illustration of the periodic spectrum and the coupling of the energy (bias field) and magnetic axes lies in the observation of repetitive weak localization. Normally, weak localization arises in disordered, low-dimensional systems when individual carrier trajectories can be scattered, by repetitive interactions with impurities, back onto their “origin.” This self-interference leads to two time reversed possible trajectories (around the closed path in ei-

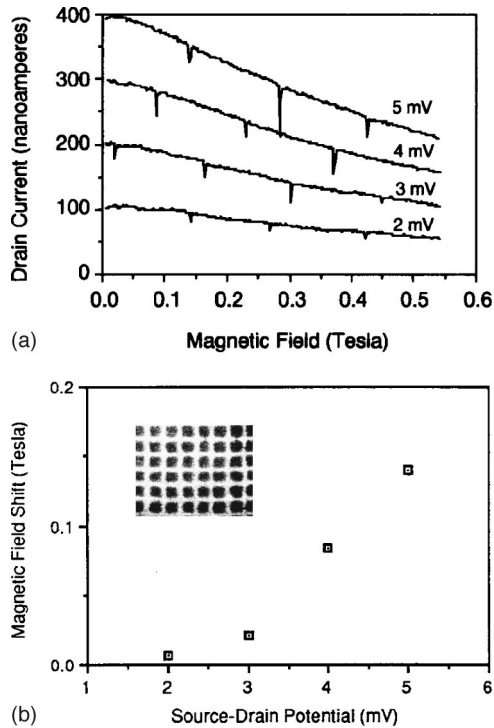


FIG. 1. (a) Current flow through a lateral surface superlattice as a function of the magnetic field normal to the transport plane. The curves are offset for clarity, and the parameter is the voltage drop per unit cell of the superlattice. (b) Main panel: the shift, away from zero magnetic field, that occurs for each gate bias. (Inset) A photomicrograph of the grid gate metallization. The period is approximately 165 nm.

ther of the two directions) that give phase interference and a reduction in the conductance. A magnetic field breaks the time-reversal invariance, and washes out the interference and the weak localization.²² In a two-dimensional lateral superlattice potential, however, the periodicity of the spectrum should provide a periodically recurring weak localization. To study this, thin 50 nm layers of GaAs, heavily doped to $1.5 \times 10^{18} \text{ cm}^{-3}$ were grown by vapor-phase epitaxy on semi-insulating GaAs substrates. A grid gate was then deposited [inset to Fig. 1(b)] to provide the superlattice potential.²³ When the gate is reversed bias near to pinchoff, there are many more ionized donors than free carriers in the channel. The confinement between the gate potential and that of the semi-insulating substrate leads to quasi-two-dimensional behavior,²⁴ and the large number of ionized donors leads to strong disorder in the transport. In Fig. 1(a), several drain current traces (offset from one another for clarity) are shown for different values of the bias drop across each unit cell of the superlattice. The sharp negative-going drops are the signal of weak localization, but they are shifted as the bias is increased. The periodicity is about 0.14 T for all curves, and this corresponds to a coupling of one flux quanta through a cell of size 170 nm, while the estimate of the actual cell size is $a \sim 165$ nm. In Fig. 1(b), the main panel shows the shift as a function of drain bias. We can understand this by noting that the electric field, arising from the bias, also contributes to the vector potential, and

$$A_y = Bx + eE\tau_m \quad (6)$$

in the Landau gauge, where τ_m is the momentum relaxation time. This leads to a change in the argument of the cosine function in Eq. (4), and

$$2n\pi\alpha \rightarrow 2n\pi\alpha - \omega_B\tau_m, \quad (7)$$

where ω_B is the Bloch frequency. Thus, the bias and the magnetic field are coupled in driving the phase in Harper's equation. It is clear from Fig. 1(b) that no shift appears until the drift velocity exceeds the Fermi velocity, or the drift energy exceeds the Fermi energy.

V. OPEN QUANTUM DOTS

The lateral superlattices above are composed of individual quantum dots connected together. The coupling between these dots can be either by tunneling, if the Fermi energy lies below the saddle energy of the potential between the dots, or by normal transport through a quantum point contact. By the latter, we mean that, even when the Fermi energy lies above the saddle of potential, only a few transverse modes can propagate between the dots. Hence, the coupling is still quantum in nature, even though it is not tunneling. For several years, we have been studying the transport in these open quantum dots, in order to ascertain the relevant physics in dots and dot arrays.²⁵ Here, we briefly discuss the fluctuations and their significance for dot-to-dot coherence and the role of the "environment" on the transport.

In Fig. 2, we show the resistance of a three-dot array as the gate voltage is varied. A photomicrograph of the dot array is shown in the upper left as an inset. At low temperature fluctuations in this resistance are seen as the bias is varied. These fluctuations are repeatable and are not noise. They arise as the bias, or an applied magnetic field is varied. In essence, the variation of either of these two quantities moves the Fermi level through the density of states of the dots. The latter is formed by the number of quantum states that exist per unit energy. Normally, one thinks that the quantum effects will wash out as the dots are opened, but this is not the case. Instead, the quantum states remain, and their broadening will depend upon their coupling to the outside world, as indicated in Eq. (2).²⁶ Each of the fluctuations corresponds to a Fano-type resonance as the Fermi energy crosses an eigenvalue. In order to compute the eigenvalues, one must include the role of the environment in this computation, as discussed above. In Fig. 3, we show a calculation for a stadium-shaped dot. Here, the Fano resonances are plotted as the Fermi energy is varied for an open dot coupled to its environment. The upper symbols indicate the states for a closed dot, while the lower symbols indicate the states that are found when the quantum point contact is included in the calculation. It is clear that only these latter states actually line up with the resonances. We have also shown, by classical simulations, that the transport is dominated by these resonances, and that they persist in the open dot due to the fact that they are only weakly coupled. In fact, we find that the classical phase space is that of a mixed system, in which an isolated Kolmogorov–Arnold–Moser (KAM) island exists (in the

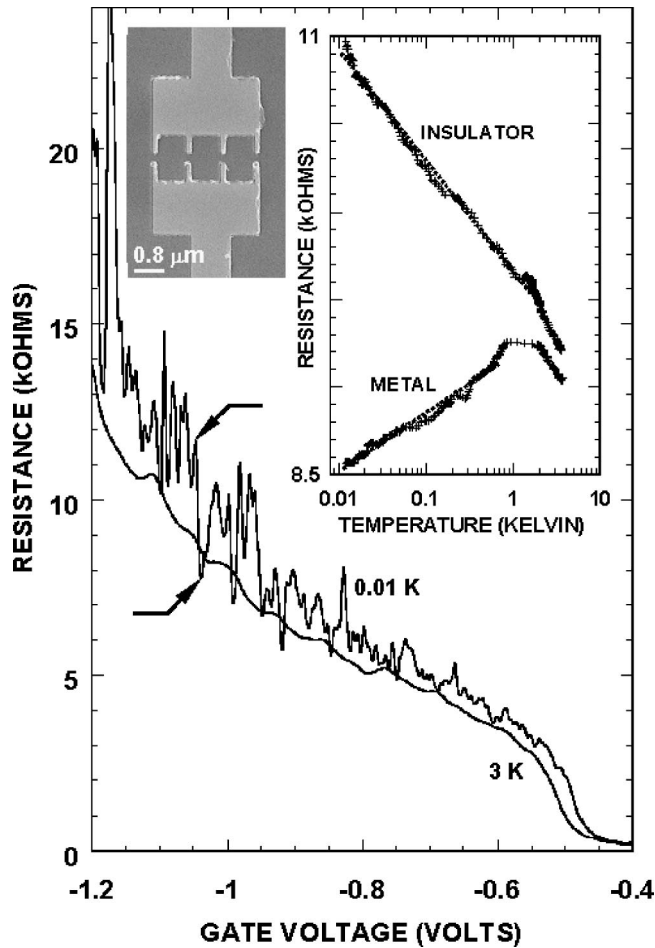


FIG. 2. (Main panel) source–drain resistance through a three dot array as a function of the bias applied to the confining gates. The smooth curve is one taken at 3 K, while the rapidly fluctuating curve is taken at 10 mK. (Upper left inset) photomicrograph of the gates which define the three dots on a GaAs/AlGaAs heterostructure. (Upper right inset) resistance of the maxima and minima as a function of temperature, illustrating the metal and insulator behavior.

phase space), whose size and orbits are determined by the quantum eigenstates.²⁷ Since the KAM island is isolated classically, transport can only occur through phase-space tunneling onto, and off of, these islands. This is why the conductance fluctuations persist even when the dot is opened, and the exact resulting eigenstates depend upon the renormalization present with this coupling, as indicated in Eq. (2).

When we have multiple dots, as in the array mentioned above, the amount of dot-to-dot coupling will vary with the gate bias. In this case, we can sense the nature of the eigenstates by varying the magnetic field—characteristic magnetic frequencies correspond to the enclosed area of the resonance in phase space (the contribution to the density of states comes from the closed orbits, both classically and quantum mechanically).²⁸ If the orbits couple between the dots in the array, we expect this to show less magnetic field will be needed to couple one flux quantum, and the magnetic frequency will be higher. Indeed, we have found this to be the case in actual experiments on dot arrays.²⁹ It is clear that coherence can exist throughout the array, and lead to coop-

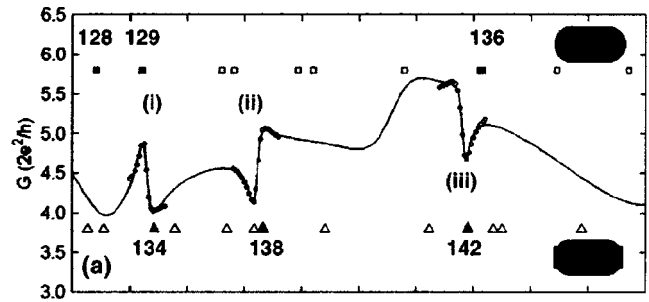


FIG. 3. Conductance through an open stadium-shaped quantum dot as a function of energy. The open and closed squares, above the curve, represent resonant eigenstates of the closed stadium pictured at the upper right corner. The open and closed triangles represent the eigenstates of the extended stadium pictured in the lower right corner. The closed symbols represent states coupled to the leads during transport.

erative effects in the transport. Indeed, such cooperative effects lead to superlattice behavior,^{30,31} as discussed above.

Finally, we turn to one last important effect. As shown in the upper-right inset to Fig. 2, each of the resistance peaks has a resistance that diverges as the temperature is reduced toward zero. On the other hand, each of the resistance minima has a resistance that tend toward zero as the temperature is reduced.³² This is indicative of a reentrant metal–insulator transition. Such transitions are common at low density in low dimensional systems, but rarely exhibit reentrant behavior. In addition, this behavior is reminiscent of that seen in single-electron tunneling into quantum dots—the Kondo effect.³³ Generally, it is felt that this will not occur in the open dots. However, the presence of the isolated KAM island in phase space means that tunneling onto and off of the island can lead to Kondo-like behavior, and this is thought to be the source of the metal-insulator behavior in these dots. We have carried out a simple computation, based upon an Anderson-like coupling, and found behavior such as that seen experimentally.³⁴ If correct, this indicates that strong electron–electron interactions exist between electrons trapped on the KAM island and those *external* to the dot itself—a strong device–environment coupling interaction. While more work needs to be done to confirm this view, the initial calculations seem to support such an interpretation.

VI. CONCLUSIONS

The central feature of transport in very-small devices is that the device microdynamics cannot be treated in isolation, but must be considered in conjunction with its environment. That is, any single device is embedded within an “environment” which consists of its own interfaces and the array of other devices to which it is connected, either by design or by accident. We have given several examples in terms of open quantum dots, quantum dot arrays, and lateral superlattices.

ACKNOWLEDGMENT

This work has been supported in part by the Office of Naval Research.

- ¹J. R. Barker and D. K. Ferry, *Solid-State Electron.* **23**, 531 (1980).
- ²D. K. Ferry, in *The Physics of Submicron Semiconductor Devices*, edited by H. L. Grubin *et al.* (Plenum, New York, 1983), pp. 503–520.
- ³D. K. Ferry, *Semiconductors* (Macmillan, New York, 1991), p. 528.
- ⁴K. Hess and P. Vogl, *Solid State Commun.* **30**, 807 (1979).
- ⁵B. T. Moore and D. K. Ferry, *J. Appl. Phys.* **51**, 2603 (1980).
- ⁶A. Hartstein, J. H. Ning, and A. B. Fowler, *Surf. Sci.* **58**, 178 (1976).
- ⁷B. T. Moore and D. K. Ferry, *J. Vac. Sci. Technol.* **17**, 1037 (1980).
- ⁸F. Stern and W. E. Howard, *Phys. Rev.* **163**, 816 (1967).
- ⁹D. K. Ferry, *J. Vac. Sci. Technol. B* **2**, 504 (1984).
- ¹⁰I. Knezevic and D. K. Ferry, *Phys. Rev. E* **66**, 016131 (2002).
- ¹¹D. K. Ferry, K. Hess, and P. Vogl, in *VLSI Electronics: Microstructure Science*, edited by N. G. Einspruch (Academic, New York, 1981), Vol. 2, pp. 68–105.
- ¹²M. V. Fischetti, D. A. Neumayer, and E. A. Cartier, *J. Appl. Phys.* **90**, 4587 (2001).
- ¹³W. J. Gross, D. Vasileska, and D. K. Ferry, *IEEE Trans. Electron Devices* **47**, 1831 (2000).
- ¹⁴T. D. Linton, Jr., S. Yu, and R. Shaheed, *VLSI Design* **13**, 103 (2001).
- ¹⁵S. Kaya, A. Asenov, and S. Roy, *J. Comput. Electron.* **1**, 375 (2002).
- ¹⁶M. J. Rack, D. Vasileska, D. K. Ferry, and M. Sidorov, *J. Vac. Sci. Technol. B* **16**, 2165 (1998).
- ¹⁷D. Hofstadter, *Phys. Rev. B* **14**, 2239 (1976).
- ¹⁸P. G. Harper, *Proc. Phys. Soc., London, Sect. A* **68**, 879 (1955).
- ¹⁹D. K. Ferry, *Prog. Quantum Electron.* **16**, 251 (1992).
- ²⁰E. Paris, J. Ma, A. M. Kriman, D. K. Ferry, and E. Barbier, *J. Phys.: Condens. Matter* **3**, 6605 (1991).
- ²¹E. Paris, J. Ma, A. M. Kriman, D. K. Ferry, and E. Barbier, in *Nanostructures and Mesoscopic Systems*, edited by W. P. Kirk and M. A. Read (Academic, Boston, 1992), pp. 311–322.
- ²²G. Bergmann, *Phys. Rep.* **107**, 3 (1984).
- ²³J. Ma, R. A. Puechner, A. M. Kriman, and D. K. Ferry, in *Localization and Confinement of Electrons*, edited by F. Kuchar, H. Heinrich, and G. Bauer (Springer, Berlin, 1990), pp. 268–274.
- ²⁴M. Pepper, *J. Phys. C* **10**, L173 (1977).
- ²⁵J. P. Bird, R. Akis, D. K. Ferry, and M. Stopa, in *Advances in Imaging and Electron Physics*, edited by P. Hawkes (Academic, San Diego, 1999), Vol. 107, pp. 1–71.
- ²⁶R. Akis, J. P. Bird, and D. K. Ferry, *Appl. Phys. Lett.* **81**, 129 (2002).
- ²⁷A. P. S. de Moura, Y.-C. Lai, R. Akis, J. Bird, and D. K. Ferry, *Phys. Rev. Lett.* **88**, 236804 (2002).
- ²⁸M. C. Gutzwiller, *J. Math. Phys.* **12**, 343 (1971).
- ²⁹M. Elhassan *et al.*, *Phys. Rev. B* **64**, 085325 (2001).
- ³⁰M. Leng and C. S. Lent, *Phys. Rev. Lett.* **71**, 137 (1993).
- ³¹R. Akis and D. K. Ferry, *Solid-State Electron.* **42**, 1297 (1998).
- ³²A. Shailos *et al.*, *Phys. Rev. B* **63**, 241302 (2001).
- ³³W. G. van der Wiel, S. de Franceschi, T. Fujisawa, J. M. Elzerman, S. Tarucha, and L. P. Kouwenhoven, *Science* **289**, 2105 (2000).
- ³⁴K. M. Indlekofer, J. P. Bird, R. Akis, D. K. Ferry, and S. M. Goodnick, *Appl. Phys. Lett.* **81**, 3861 (2002).